Design of a Multivariable Pole-Placement Controller for the Primary Mirror of the 10m Grantecan Telescope

L. Acosta, M. Sigut[†], A. Hamilton, J.A. Méndez, G.N. Marichal and L. Moreno
Dep. of Applied Physics, University of La Laguna, 38271 La Laguna
Tenerife, Spain

Abstract

In the design of a telescope the most important specification is to obtain a quality in the images as high as possible. The Gran Telescopio de Canarias (GTC) has got a 10m diameter primary mirror, which is segmented in 36 hexagonal pieces. This paper presents a multivariable controller for the primary mirror based on a local-global strategy. This means that the command sent to the segments will have a local contribution (using information of the own segment) and a global contribution (using information of the whole mirror). The goal of the control process is to keep the 36 segments which form the primary mirror always on a paraboloidal surface. The controller design process has been fundamental to know in detail the system dynamics features in the sense of symmetries and the coupling existing in the primary mirror of the GTC. The requirements about the sampling frequencies have also been studied. This work is the result of a collaboration between the GRANTECAN, S.A. Company and the Group of Computers and Control of Departament of Applied Physics of La Laguna University.

1 Introduction

The primary mirror of the GTC is a 10 meter diameter mirror. Due to its great size it has been segmented in 36 hexagonal pieces. There exist important advantages in the construction of a big segmented mirror instead of a monolithic one (i.e., formed from an only piece of mirror). Some of these advantages are: a smaller total weight, a lower cost, an easier construction and assembly in the place where the telescope will be placed, an easier maintenance, etc. The hexagonal segmentation has been chosen in this case. The criterion followed to choose the number of segments has been to use the largest ones within the capacities of potential polishers at reasonable prices. This limit has been set at 2.0m, which means that the smallest possible number of segments is 36 (Álvarez et al, 1997). Due to the segmentation of the GTC primary mirror, an appropriate control system must be implemented. All the segments must be on a paraboloidal surface to obtain the necessary final quality in the images they provide. The GTC is a greatly multivariable system and, because of this, the controller design process is certainly complex (Patel, 1981).

'Keck' is the name of a telescope placed in Hawaii, whose features are similar to the GTC ones (Aubrun, 1985). In this case, an integral controller combined with physical ties allow to obtain the desired performance. In this paper, a multivariable controller for the GTC, consisting of a pole-placement design, is presented.

[*] Supported by GRAN TELESCOPIO CANARIAS, S.A. Company.
[†] Email: *marsigut@ull.es*.

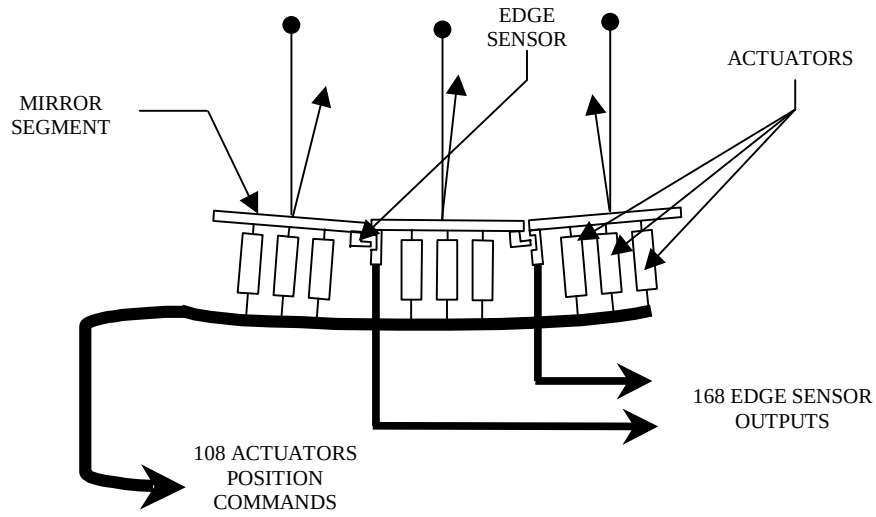

Fig.1. Representation of some actuators and sensors of the GTC primary mirror.

2 Primary Mirror Design and Dynamics

Each segment of the GTC is provided with 3 actuators and a variable number of sensors that oscillates between 3 and 6, depending on the location of the segment into the mirror. As shown in Fig. 1, the actuators are mechanical devices used to move the segments. On the other hand, the sensors measure the relative distance between two adjacent segments. Therefore, there are two sensors in each edge which is common to two segments, **a** and **b**. One of the sensors belongs to the segment **a** and the other one belongs to the segment **b**. Fig. 2 shows the structure of the 36 segments with their actuators and sensors. It can be seen than there are segments with 6, 5, 4 and 3 sensors, depending on the place where they are located into the structure. In short, the primary mirror of the telescope is provided with 108 actuators and 168 sensors.

The primary mirror of the GTC is a large scale system (Jamshidi, 1983). Its dynamics has been modeled in the state-space representation, like a system with 708 states, 108 inputs and 168 outputs. The inputs are the commands which are sent to the actuators to move the segments, and the outputs are the measurements of the sensors. At this point, it is important to notice that there are three different elements in the system, each one of them provided with a different dynamics:

- the structure which supports the primary mirror,
- the segments,
- the actuators.

In a first stage, if the actuators are considered as ideal devices (with no dynamics and no delays), a system with 276 states is obtained, instead of the 708 states which describe the whole system. In this case we only take into account the structure and segments dynamics. The behavior of the real actuators is described by the following expression, where $\overline{q}_i$ is the command applied and q_i the corresponding actuator response:

$$q_i = \frac{e^{-s\tau_q}}{1+\xi_q \frac{s}{w_q}+\frac{s^2}{w_q^{\,2}}}\,\overline{q}_i \qquad (1)$$

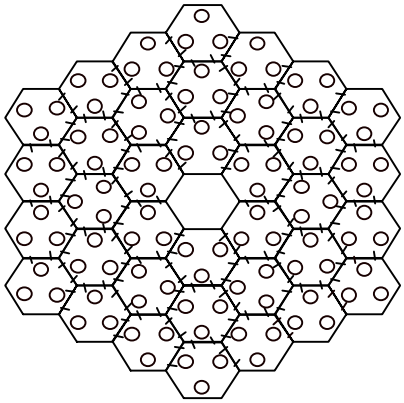

Fig.2. Primary mirror of the GTC with the 36 segments, the 108 actuators (o) and the 168 sensors (–).

being $w_q = 2\pi \times 60 sg^{-1}$, $\xi_q = 1/\sqrt{2}$ and $\tau_q = 0.5ms$. The exponential term which appears in the numerator corresponds to the actuator time delay. The second order Padé approximation is used.

The 708 states of the system are:

a : dominant modes of the structure which supports the primary mirror (30).

$\dot{a}$: time derivatives of these modes (30).

x_e : distances from the actuators to the cell (108).

$\dot{x}_e$: time derivatives of these states (108).

$r1$: first state associated with the time delay for each actuator (108).

$r2$: second state associated with the time delay for each actuator (108).

q : first state associated with the actuators dynamics (108).

$\dot{q}$: second state associated with the actuators dynamics (108).

The matrix state-space equations which describe the system dynamics are the following ones:

$$\frac{d}{dt}\begin{bmatrix} a \\ \dot{a} \\ xe \\ m_s \dot{x}e \\ r1 \\ r2 \\ q \\ \dot{q} \end{bmatrix} = \mathrm{A}\begin{bmatrix} a \\ \dot{a} \\ xe \\ m_s \dot{x}e \\ r1 \\ r2 \\ q \\ \dot{q} \end{bmatrix} + \mathrm{B} * U + \begin{bmatrix} 0_{30\times1} \\ 0_{30\times1} \\ 0_{108\times1} \\ P \\ 0_{108\times1} \\ 0_{108\times1} \\ 0_{108\times1} \\ 0_{108\times1} \end{bmatrix} \quad ; \quad S = \mathrm{C} * \begin{bmatrix} a \\ \dot{a} \\ xe \\ m_s \dot{x}e \\ r1 \\ r2 \\ q \\ \dot{q} \end{bmatrix} + \mathrm{D} * U \qquad (2)$$

being

$$A = \begin{bmatrix}
0_{30\times30} & I_{30\times30} & 0_{30\times108} & 0_{30\times108} & 0_{30\times108} & 0_{30\times108} & 0_{30\times108} & 0_{30\times108} \\
-W^2 - k_s V^T V & -C - c_s V^T V & k_s V^T & \frac{c_s}{m_s} V^T & 0_{30\times108} & 0_{30\times108} & -k_s V^T & -c_s V^T \\
0_{108\times30} & 0_{108\times30} & 0_{108\times108} & \frac{1}{m_s} I_{108\times108} & 0_{108\times108} & 0_{108\times108} & 0_{108\times108} & 0_{108\times108} \\
k_s V & c_s V & -k_s I_{108\times108} & -\frac{c_s}{m_s} I_{108\times108} & 0_{108\times108} & 0_{108\times108} & k_s I_{108\times108} & c_s I_{108\times108} \\
0_{108\times30} & 0_{108\times30} & 0_{108\times108} & 0_{108\times108} & 0_{108\times108} & I_{108\times108} & 0_{108\times108} & 0_{108\times108} \\
0_{108\times30} & 0_{108\times30} & 0_{108\times108} & 0_{108\times108} & -\frac{8}{T^2} I_{108\times108} & -\frac{4}{T} I_{108\times108} & 0_{108\times108} & 0_{108\times108} \\
0_{108\times30} & 0_{108\times30} & 0_{108\times108} & 0_{108\times108} & 0_{108\times108} & 0_{108\times108} & 0_{108\times108} & I_{108\times108} \\
0_{108\times30} & 0_{108\times30} & 0_{108\times108} & 0_{108\times108} & w_q^2 I_{108\times108} & 0_{108\times108} & -w_q^2 I_{108\times108} & -2\xi_q w_q I_{108\times108}
\end{bmatrix}$$

$$B' = \begin{bmatrix} 0_{108\times30} & 0_{108\times30} & 0_{108\times108} & 0_{108\times108} & -\frac{8}{T} I_{108\times108} & \frac{32}{T^2} I_{108\times108} & 0_{108\times108} & w_q^2 I_{108\times108} \end{bmatrix}$$

$$C = \begin{bmatrix} 0_{168\times30} & 0_{168\times30} & M & 0_{168\times108} & 0_{168\times108} & 0_{168\times108} & 0_{168\times108} & 0_{168\times108} \end{bmatrix}$$

$$D = 0_{168\times108}$$

where:

- ***V(*** $\mathbf{108\times30}$ ***)***: the cell modal displacements matrix.
- ***W(*** $\mathbf{30\times30}$ ***)***: the angular modal frequencies diagonal matrix.
- **C(** $\mathbf{30\times30}$ **)**:the damping diagonal matrix ($c_i = 2\xi_i w_i$, ξ_i = damping relative to the ***i*** mode).
- $\mathbf{k_S = 6N/mm}$: segments base stiffness.
- $\mathbf{c_S = 2000kg/sg}$: segments base damping.
- $\mathbf{m_S = 180kg}$: segment mass associated with one of its three actuators.
- $\mathbf{w_q = 2\pi\times60sg^{-1}}$: actuators natural frequencies.
- $\boldsymbol{\xi_q = 1/\sqrt{2}}$: actuators damping.
- $\mathbf{T = 5ms}$: actuators time delay.
- **P(** $\mathbf{108\times1}$ **)**: disturbances caused by the wind (only affect the $\dot{x}_e$ states).
- **M (** $\mathbf{168\times108}$ **)**: geometric relationship between the actuators position and the sensors signals.

And where $0_{m\times p}$ and $I_{n\times n}$ represents the null *m×p* matrix and the *n×n* identity matrix, respectively. Fig. 3 shows the block diagram of the open loop system.

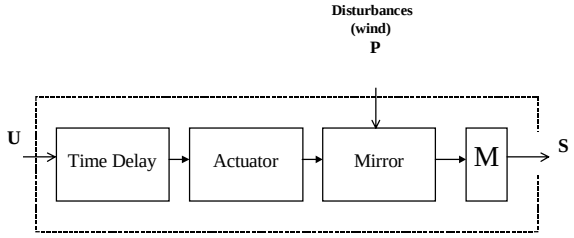

Fig.3. Block diagram of the open-loop system.

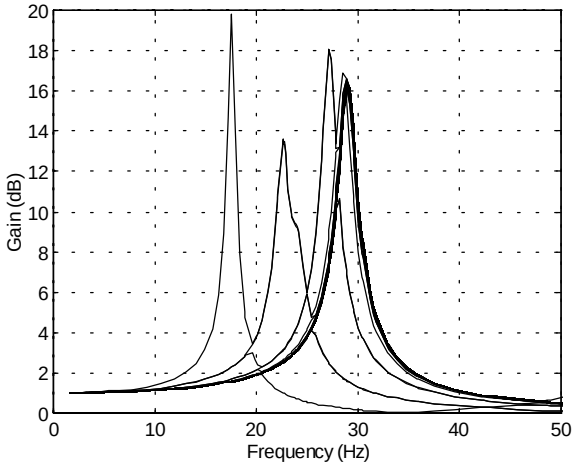

Fig. 4. System singular values in the frequency domain.

3 Open-Loop Response

It is important to know how the open-loop system response is to compare it with the closed-loop one. Fig. 4 shows the system response in the frequency domain (Klema, 1980). Fig. 5 shows the open-loop time response of the primary mirror actuators when they start from positions which are not the equilibrium ones. In both figures it can be seen that the system dominant frequencies are 28Hz, which corresponds to the segments dynamics, and 17Hz, which is the first structure mode. On the other hand, the other conclusion we can extract from Fig. 5 is that the system takes more than 1 second to reach the equilibrium position. The coupling between the segments through the structure which supports them is an effect which plays a fundamental role in the system response. Fig. 6 shows the open-loop time response of the actuators when all of them are initially in their equilibrium point except three of them (the three actuators of a segment). It can be seen that only one of the segments can move the other 35.

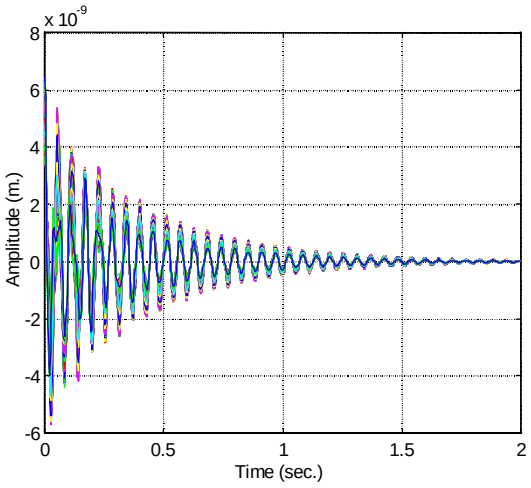

Fig. 5. Open loop system time response.

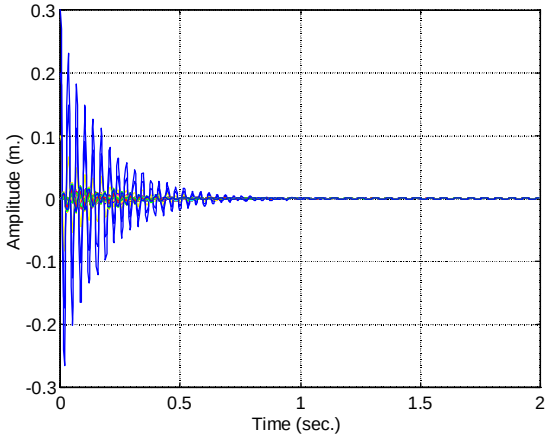

Fig. 6. Time response of the open loop system with act.49: 0.1m., act.54: 0.2m, act.102: 0.3m. at t=0sec.

4 Controller Design

The specifications of the pole-placement controller for the primary mirror of the GTC are:

1) to guarantee that the segments will reach the desired final position with a bandwidth as high as possible.

2) to eliminate, or at least to reduce, the frequency of the dominant oscillations of the system.

3) to comply with the restrictions imposed by the system geometry.

In this first study, effects like wind disturbances, measurement noise, actuation noise and non-modeled dynamics have not been considered. The only noises taken into account are spurious effects which deviate the segments from their equilibrium position. The pole-placement controller has been designed in accordance with a strategy consisting of two levels of control: local and global. In this control structure there is a computer for each one of the segments which computes the commands for its actuators. At the same time, other computer has to calculate the global commands using the 36 segments information. The reason why a local-global strategy could result more interesting is because the local control can be applied at a frequency much higher than the global one. This is because to calculate the global command is necessary to know the signals of the 168 sensors; on the contrary, to obtain the local command for the 3 actuators of a segment it is enough to know the measurements of 3 of its sensors. In accordance to this dual strategy the following pole-placement controller has been designed

$$U = -Kl * S - Fl * \dot{S} - Kg * x - Fg * \dot{x} \tag{3}$$

being

$S(168\times 1)$: the 168 sensors measurements.

$x(708\times 1)$: the system state vector.

$Kl(108\times 168), Fl(108\times 168)$: local controller matrices.

$Kg(108\times 708), Fg(108\times 708)$: global controller matrices.

$U(108\times 1)$: the commands which will be applied to the 108 actuators.

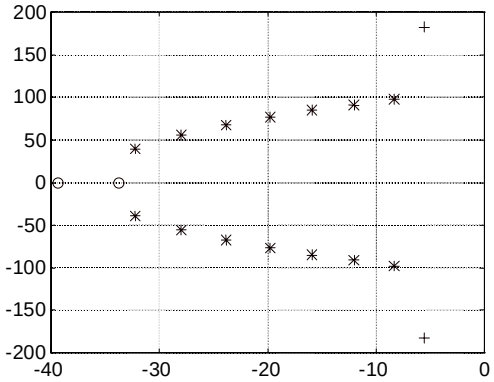

Fig. 7. Evolution of the dominant system poles when different pole-placement controllers are applied.

It is important to notice two things: **a)** *Kl*, *Fl*, *Kg* and *Fg* can be computed off-line, so the only on-line calculus is the matrices product in eq. (3), and **b)** although *Kg* and *Fg* are (108×708) matrices, the columns which do not correspond to the actuators position (*xe* states) are equal to zero.
The control command can be divided into a local one and a global one. The local controller has got the following form:

$$U = -Kl * S - Fl * \dot{S} \tag{4}$$

This action is the responsible for eliminating the coupling between the 3 actuators of a segment and for changing the segments dynamics. We want that the poles which describe this dynamics to be as close as possible to the real axis (to reduce the oscillations frequency) and to have a negative real part as high as possible (to increase the system bandwidth). Due to the important symmetries present in the system, the position of these poles will depend on two only scalar parameters called *vk* and *vf*. To obtain the closed-loop matrix and, consequently, its poles positions, the appropriate elements must be equal to *vk*, *vf*, and some multiples of these vales (due to the simmetries). Thus, Fig. 7 shows with '+' the position of the open-loop (*vk=0*, *vf=0*) segment poles in the complex plane. Varying *vk* and *vf* these poles move to the positions marked with '*'; finally, when *vk=-1500* and *vf=-0.044*, we have the poles in the desired position ('o'). To explain briefly how *Kl* and *Fl* are tuning, we will work with the subsystem corresponding to one of the segments. It is described, in the state-space representation, by 18 states (where only the segment and its actuators dynamics has been considered, but not the structure modes). The matrices associated with this subsystem are called *ad*, *bd* and *cd* (the *d* matrix is zero). Fig. 8 shows the non-zero elements of *ad* and it can be seen that the symmetries in the segment are obvious. The local command applied to the segment actuators is:

$$U = -kl * S - fl * \dot{S} \tag{5}$$

being *kl* and *fl* 3×3 matrices.
In this case, the closed-loop matrix is the following:

$$H = (I_{18\times 18} + bd * fl * cd)^{-1} * (ad - bd * kl * cd) \tag{6}$$

If $fl = 0_{3\times 3}$ this matrix becomes:

$$H = ad - bd * kl * cd \tag{7}$$

Applying to the closed-loop system the considerations about dynamics and cancellation of the coupling between the actuators, the following equations are obtained:

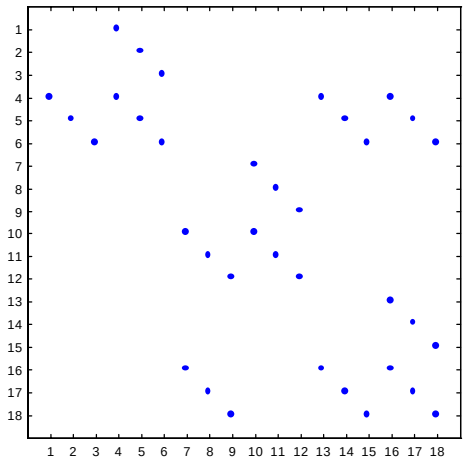

Fig. 8. Non-zero elements of a segment matrix *ad*.

$$\begin{bmatrix} h_{7,1} & h_{7,2} & h_{7,3} \end{bmatrix} = \begin{bmatrix} vk & 0 & 0 \end{bmatrix} \tag{8}$$

$$\begin{bmatrix} h_{8,1} & h_{8,2} & h_{8,3} \end{bmatrix} = \begin{bmatrix} 0 & vk & 0 \end{bmatrix} \tag{9}$$

$$\begin{bmatrix} h_{9,1} & h_{9,2} & h_{9,3} \end{bmatrix} = \begin{bmatrix} 0 & 0 & vk \end{bmatrix} \tag{10}$$

to calculate kl.

To determine *fl* we assume that $kl = 0_{3\times3}$, so:

$$H = (I_{18\times18} + bd * Fl * cd)^{-1} * ad \tag{11}$$

and we obtain a new set of equations:

$$\begin{bmatrix} h_{7,4} & h_{7,5} & h_{7,6} \end{bmatrix} = \begin{bmatrix} vf & 0 & 0 \end{bmatrix} \tag{12}$$

$$\begin{bmatrix} h_{8,4} & h_{8,5} & h_{8,6} \end{bmatrix} = \begin{bmatrix} 0 & vf & 0 \end{bmatrix} \tag{13}$$

$$\begin{bmatrix} h_{9,4} & h_{9,5} & h_{9,6} \end{bmatrix} = \begin{bmatrix} 0 & 0 & vf \end{bmatrix} \tag{14}$$

to calculate fl.

Once we have found the *kl* and *fl* 3×3 matrices corresponding to the 36 segments it is immediate to construct the *Kl* and *Fl* 108×168 matrices corresponding to the whole system. We only have to put the elements of the 3×3 matrices in the adequate positions into the 108×168 matrices.

We have just seen how the application of an adequate local command could eliminate the coupling between the actuators of a segment. However, the coupling between the different segments of the GTC primary mirror is an effect which can not be treated locally. If we only apply a local command we find that the system becomes unstable, so we must design a global controller to decouple the segments. This controller has got the following form:

$$u_{global} = -Kg * x - Fg * \dot{x} \tag{15}$$

The closed-loop matrix which results from the application of a local command of the form showed in eq. (4) is:

$$H = (I_{708\times708} + B * Fl * C)^{-1} * (A - B * Kl * C) \tag{16}$$

To know which of this matrix elements are coupling ones we can realign the system states to have a new matrix *A*' formed by 18×18 boxes, each one of them corresponding to one of the mirror segments. If the elements out of these boxes are zero, the full matrix eigenvalues (system poles) will coincide with the boxes poles (which have been set by the local controller). Once we know which elements must be canceled the process of design of *Kg* and *Fg* has got a simple goal. When we apply a global command ($-Kg*x-Fg*\dot{x}$), the value of the coupling elements in the closed-loop matrix must be the same, with the contrary sign, as the value obtained when we apply the local command ($-Kl*S-Fl*\dot{S}$).
In conclusion, the pole-placement controller designed for the GTC primary mirror has the form showed in eq. (3) and it can be seen that the resulting closed-loop matrix:

$$H=(I_{708\times708}+B*Fl*C+B*Fg)^{-1}*(A-B*Kl*C-B*Kg) \tag{17}$$

is stable. Also, the poles which describe the segments dynamics are in the positions determined by *vk* and *vf*. At this point it results appropriate to notice that although it is not generally acceptable to use the derivative of the system state in the feedback law because of noise signal amplification, this is not a problem in our case. The main noise source present in the GTC primary mirror is the wind effect and it is a low frequency signal (≈30Hz). Because of this, the sampling frequency will be always much higher than the noise one and there will not be problems with its amplification. However, it is possible to avoid the problems caused by the estimation of the derivatives. If *vf*=0, the control law has got the following form:

$$U=-F*S-K*x \tag{18}$$

The results obtained with this controller and with the one in eq. (3) can then be compared.

5 Results

Once the pole-placement controller for the GTC primary mirror has been designed, the next step is to check how good it is by means of simulation. In all the simulations presented in this chapter the actuators are initially in the same positions as in Fig. 5. Fig. 9 shows the results of the simulation when *vk*=-1500, *vf*=-0.044 and local and global control frequencies are 1000 and 500Hz, respectively.

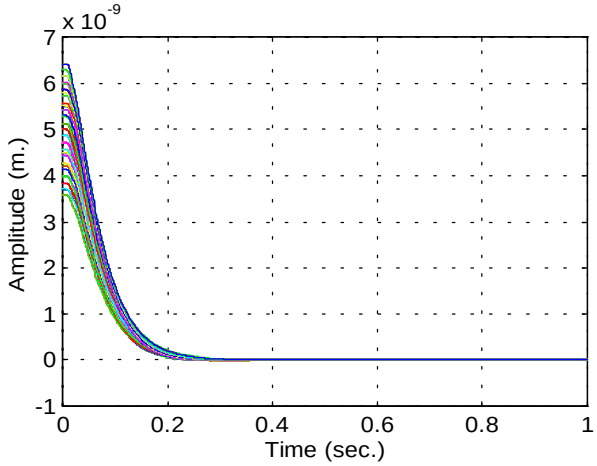

Fig. 9. Time response of the actuators when local frequency is 1000Hz and the global frequency is 500Hz, with *vf*=-0.044.

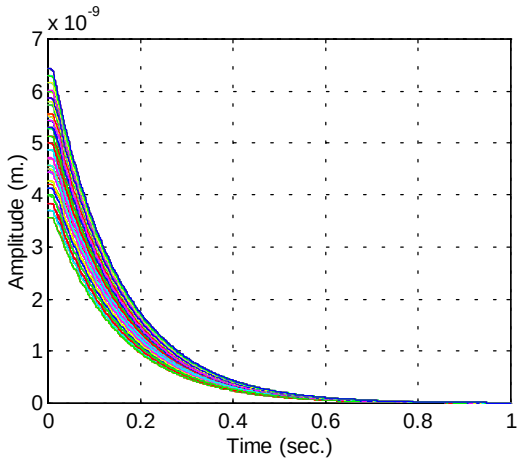

Fig. 10. Time response of the actuators when local frequency is 1000Hz and the global frequency is 500Hz, with *vf*=0.

Fig. 10 shows the same simulation taking *vf*=0. It can be seen that only when *vf*≠0 the 17Hz and 28Hz oscillations disappear completely. For smaller frequencies and *vf*≠0, the oscillations amplitude grows up and it is also a bit higher when *vf*=0. With respect to the system response speed, in the cases simulated it becomes faster than without control action. However, the actuators reach their equilibrium position quite faster when *vf*≠0. In Table 1 we present the settling time for every case.

6 Conclusions

A pole-placement controller for the primary mirror of the GTC has been proposed and tested in this paper. The goals proposed in the design stage, which were to reduce the frequency of the dominant system oscillations and to obtain a bandwidth as high as possible, have been reached. The existence of important symmetries in the system, as shown in Fig. 8, has played a fundamental role in the controller design process. It has made possible with a quite simple method a process which would have been practically unapproachable from a mathematical point of view, due to the large dimensions of the system. However, this controller has been designed in absence of noise whose main contribution comes from the wind effect. The other important factor which has not been taken into account are the differences between the model that has been used to design the controller and the real system dynamics. So, the next step will be to design a controller which guarantees that it will be robust not only in the case of changes in the system dynamics model, but also against the different noise sources.

References

P. Álvarez et al (1997). *Gran Telescopio Canarias, Conceptual Design*.

K. J. Aström and B. Wittenmark (1997). *Computer Controlled Systems*, Prentice Hall.

J. N. Aubrun, K. R. Lorell, T. W. Havas and W. C. Henninger (1985). *An analysis of the segment alignment control system for the W.M. Keck Observatory Ten Meter Telescope - Final Report.*

M. Jamshidi (1983). *Large Scale Systems Modelling and Control*, Nort-Holland.

Virginia C. Klema and Alan J. Laub (1980). "The Singular Value Descomposition: Its Computation and Some Applications," *IEEE Transactions on Automatic Control*, Vol. AC-25, no. 2, pp. 164-176.

R. Patel and N. Munro (1981). *Multivariable Control: Theory and Design*, Pergamon Press.

Vf	**Local control frequency (Hz)**	**Global control frequency (Hz)**	**Settling time (sc)**
-0.044	1000	500	≈0.35
0	1000	500	≈0.9
-0.044	200	100	≈0.8
0	400	200	≈1.0

Table 1: Settling time for some of the cases simulated.